韓國海岸海洋工學發表論文集 (2003)
第14券, pp. 344-352

On the Behavior of Suspended Sediment near a Silt Screen and the Screen Efficiency in a Microtidal Coastal Area

Jae Youll Jin[1], Won Oh Song[1], Jin Soon Park[1], Jang Won Chae[1],
Sung Eun Kim[1], Weon Mu Jeong[1], Ki Dai Yum[1] and Jae Kyung Oh[2]

1. INTRODUCTION

Sediment plumes arising from various coastal works can cause detrimental effects on the coastal ecosystem in various manners.

Although the most active countermeasure against the plumes is to restrict the works to specified time periods known as *environmental windows* (Reine et al., 1998), silt screens have been widely used for reducing the spreading of suspended sediments (SS) generated by coastal works.

However, it has been recognized that the performance of a silt screen is limited by certain conditions including current speed, wave height, and dredger type etc., which means that if not carefully designed and applied the screen will disturb the seafloor and cause sediment resuspension (Ooms, 1997). Furthermore, the net effect may even be detrimental (Shaw et al., 1998). Hence, the use of silt screens is not always practical or economic, and expert attention is needed during their design and use. The additional cost and problems presented by the use of silt screen mean that other environmental measures can frequently be more suitable (John et al., 2000).

Thus it may be desirable to carry out a pilot test as Penny's Bay Development in Hong Kong (Mouchel Asia Ltd., 2002) to check whether the silt screen achieves the expected performance especially in the construction projects of long-term and large dimension.

However, without a quantitative consideration of the efficiency, Korean regulators have requested to use silt screens in almost all coastal works having any potential to increase suspended sediment concentration (SSC).

In order to assess the mitigation efficiency of a traditional silt screen of fixed hanging type, intensive field measurements were carried out in the area of Busan New Port being constructed at a southeastern tip of Korea.

2. FIELD MEASUREMENTS

Coastal area around Busan New Port where large dimension of a total of 63.6 million m^3 has being dredged for the construction is shown in Fig. 1.

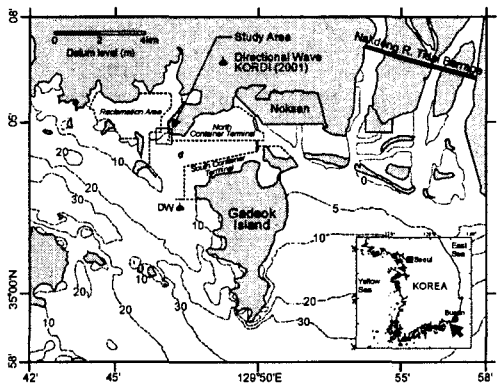

Fig. 1. Location map of Busan New Port under construction and the study area.

[1] Corresponding Author : Jae-Youll Jin, Coastal and Harbor Engineering Laboratory, Korea Ocean Research and Development Institute, Ansan, Seoul 425-600, Korea, jyjin@kordi.re.kr

[2] Department of Oceanography, Inha University, Incheon 402-751, Korea

Table 1. Working periods and dredged volumes of target dredgers

Period	Dredger	Dredged Volume (m^3)
08:00-20:00 July 5	Backhoe (3.5m^3)	1,000
08:00-14:00 July 6	Backhoe (3.5m^3)	500
07:00-18:00 July 8	Backhoe (3.5m^3)	500
07:00-18:00	Grab (4m^3)	500
04:00-24:00	Grab (8m^3)	2,000
07:00-18:00 July 9	Backhoe (3.5m^3)	500
07:00-18:00	Grab (4m^3)	500
04:00-24:00	Grab (8m^3)	2,000
07:00-18:00 July 10	Backhoe (3.5m^3)	500
07:00-18:00	Grab (4m^3)	500
04:00-24:00	Grab (8m^3)	1,500
07:00-18:00 July 11	Backhoe (3.5m^3)	500
07:00-18:00	Grab (4m^3)	500
07:00-18:00 July 12	Grab (4m^3)	500

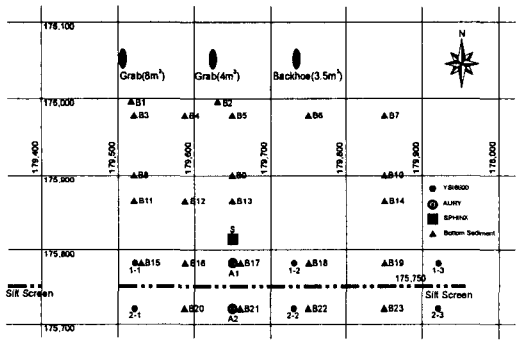

Fig. 2. Location map of field measurements in TM coordinates.

During the working period of three mechanical dredgers (Table 1) in the study area shown in Fig. 1, field measurements were carried out to assess the efficiency of a silt screen (Fig. 2).

Working area of each dredger in longitudinal and latitudinal directions were approximately 20 m and 110 m, respectively. At a distance of 220 m to 330 m southward from the dredgers, silt screens of fixed hanging type had been installed. The screen and water depths were 3 m and about 5.5 m, respectively. The spring rise at the Gadeok Tidal Station near to the study area is 1.8 m.

Bottom sediments were sampled at 23 positions (B# in Fig. 2). SSC, water depth, current velocity and direction at 3 m above the bed (mab) of site A1 (July 5-8, 2001) and A2 (July 5-11, 2001) were measured every five minutes with sediment flux monitoring systems (AURYs) consisting of 8 automatic water samplers of Auttles (Jin et al., 2003a), a multi- parameter monitor of YSI6600 and current meter of RCM9.

A benthic boundary layer monitoring system, SPHINX (KORDI, 2000), deployed at site S measured current velocity and optical turbidity at 25, 30 and 50 cm above the bed (cmab) as well as wave characteristics with acoustic velocimenters (VECTORs) of Nortek, optical backscattering sensors (OBS-3s) of D&A Instrument Co. from July 7 to 11, 2001.

Additionally, SSC profiles were measured at 6 sites 1-1 to 2-3 with a YSI6600 on July 10.

3. RESULTS

3.1 Bottom Sediments

Particle compositions and their statistical parameters at the 23 sites are presented in Table 2. The mean diameters (d_m) are about 5ϕ (31.3μm) to 6ϕ (15.6μm) except for a few sites. The difference of d_m at B17 and B21 may result in the difference of SSC at A1 and A2 in some degree. The standard deviations (σ) ranging about 2 to 4 mean the bed materials are very poorly sorted.

Table 2. Particle composition of bottom sediments and the statistical parameters by moment method

Station B#	Weight composition(%)				d_m (ϕ)	σ (ϕ)	S_k	K_t
	Gravel	Sand	Silt	Clay				
1	1.3	23.1	53.9	21.6	5.7	2.8	-0.5	2.6
2	4.6	27.2	46.8	21.5	5.2	3.3	-0.4	2.2
3	1.0	31.7	50.8	16.5	5.3	2.7	-0.1	2.5
4	18.7	41.4	29.5	10.4	2.9	3.7	0.2	1.9
5	0.0	15.8	59.8	24.5	6.3	2.3	-0.3	2.8
6	0.1	41.8	46.9	11.2	4.8	2.3	0.6	3.1
7	4.9	24.3	52.6	18.3	5.2	3.1	-0.5	2.8
8	0.2	15.3	62.7	21.7	6.4	2.1	-0.3	3.0
9	0.0	32.9	54.2	12.9	5.2	2.2	0.6	2.7
10	2.1	36.2	46.9	14.8	4.7	3.1	-0.1	2.1
11	0.0	17.1	62.1	20.9	6.1	2.2	0.0	2.7
12	4.0	24.0	51.7	20.3	5.4	3.1	-0.5	2.5
13	0.0	40.6	47.4	12.0	4.8	2.5	0.2	2.7
14	0.7	29.8	55.2	14.2	5.2	2.4	0.2	2.9
15	0.0	19.7	60.2	20.1	6.0	2.2	0.2	2.4
16	0.0	23.3	57.9	18.8	5.8	2.4	-0.1	2.7
17	1.3	60.2	33.2	5.3	3.9	2.0	0.8	5.1
18	2.3	44.1	39.8	13.8	4.3	3.2	0.1	1.9
19	4.6	59.8	26.5	9.1	3.1	3.2	0.6	2.3
20	4.9	38.5	45.9	10.8	4.5	2.7	-0.2	3.6
21	0.0	16.6	60.7	22.8	6.1	2.5	-0.4	3.0
22	1.2	35.1	49.0	14.7	5.0	2.6	0.1	2.7
23	0.0	12.4	63.9	23.7	6.4	2.1	-0.1	2.7

3.2 Tidal Currents and SSC

After in-situ calibration of the OBS turbidity in nephelometric turbidity unit (NTU) measured by the YSI6600s to SSC with the seawater concurrently sampled by the Auttles (Fig. 3), temporal variations of current speed, direction and SSC at 3 m above the bed of sites A1 and A2 are shown in Fig. 4. Fig. 4b shows the data at only A2 because the AURY at A1 was retrieved on July 8.

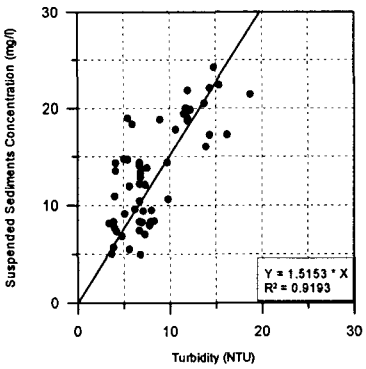

Fig. 3. Correlation between OBS turbidity and SSC.

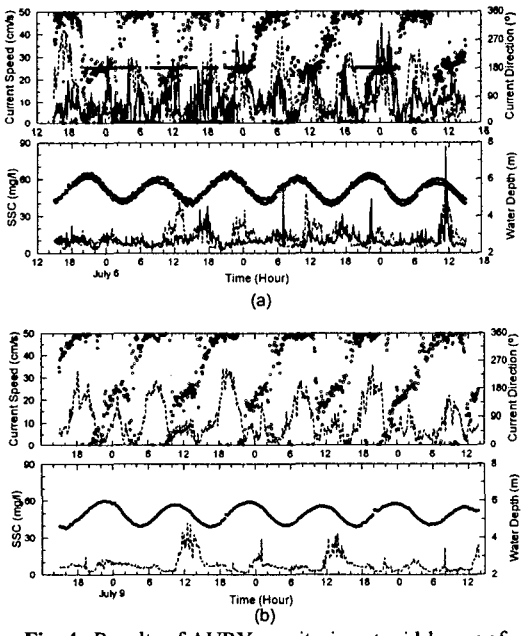

Fig. 4. Results of AURY monitoring at mid-layers of A1 and A2; filled (A1) and open (A2) circles are current direction and water depth, solid (A1) and dotted (A2) lines are current speed and SSC, respectively.

Maximum speeds of northward flood currents at A1 and A2 are about 25 cm/s and 40 cm/s, respectively, while those of southward ebb currents 40 cm/s and 25 cm/s vice versa. This means the speed of mid-layer at the downstream of the screen is weaker than that at the upstream. Considering the relatively short distance of about 60 m between A1 and A2, these temporal variations may not be local characteristics but caused by the screen.

SSC varies from about 5 to 90 mg/l. Dredging-induced plumes can directly influence the SSC of A1 and A2 only during ebb period. Thus, considering the SSC in the period to 08:00 July 6 when only the backhoe dredger was working during flood tides, it can be said that background SSC around the study area ranges 5 to 20 mg/l.

However, from 09:00 on July 6 to 04:00 on July 8, the peaks occurred even during flood tides. Furthermore, SSC at A2 being farther from the dredging sites is higher than that at A1 during ebb period. Neither dredging operation nor normal condition without dredging can explain these abnormally considerable SSC especially on July 7 when none of the dredgers worked. Hence, more detail discussions are required.

It is believed that the SSC peaks in ebb periods after about 10:00 on July 8 reflect the sediment plumes generated by the dredging. SSC at A1 increases up to about 90 mg/l during the last ebb period in Fig. 4a when

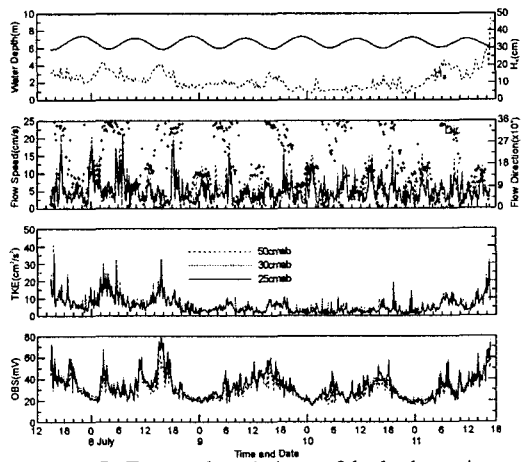

Fig. 5. Temporal variations of hydrodynamic parameters and OBS voltage at 3 near-bed layers at site S.

all the 3 dredgers were working, while the peak at A2 is about 40 mg/l. Sudden drop of the SSC at A2 at about 01:00 on July 10 in ebb period seems to be due to the closing of the $8m^3$ dredger's single work.

Currents and OBS voltage at 3 near-bed layers of site S are shown in Fig. 5 with water depth, significant wave height and turbulent kinetic energy (TKE) computed with 3-dimensional current velocity of 8 Hz.

The magnitudes of current speeds at 25, 30 and 50 cmab are about the same, the maximum of which is about 20 cm/s. The distance between sites S and A1 was only about 30 m . Thus, it may be expected that the ebb currents are stronger than the flood at S as site A1. On the contrary, however, most of flood peaks are rather higher.

The magnitudes of OBS voltages at the three layers are also about the same although that of the lowest layer is slightly higher. Unfortunately, the OBSs were not calibrated in situ. However, assuming that the size distribution of suspended particles at S is similar to that at A1, and then applying the manufacturer's calibration result relating 5 volts to 2,000 NTU and the correlation formula in Fig. 3, the minimum of about 20 mV and the maximum of about 80 mV in Fig. 5 can be related to about 12 mg/l and 50 mg/l, respectively. Referring to the minimum SSC at sites A1 and A2, the results of this indirect calibration seem to be reasonable. In this estimation, however, it should be cautious that the OBS gain (volts per mg/l) varies by a factor of 200 with particle size (D&A Inst. Co., 1991), which means that the SSC at S is much higher than the estimation if the suspended grains are coarser than those at A1 and A2.

In the period from about 04:00 on July 8 to 24:00 on July 10, the OBS turbidity in voltage varies with dredging production and tidal phase. The major peaks are associated with the ebb period when all the dredgers were working. Before and after the period, however, OBS turbidity has closer relationship with TKE, which must be caused by waves.

SSC profiles at the paired front and rear sites during ebb period are shown in Fig. 6. Although there are time gaps of 5 to 14 minutes between the paired profiles due to unsynchronized monitoring, it must be noted that most of SSC at the downstream sites 2-1, 2-2 and 2-3 are rather higher than those at the upstream. Additionally, the vertical gradients of SSC in shallower and deeper

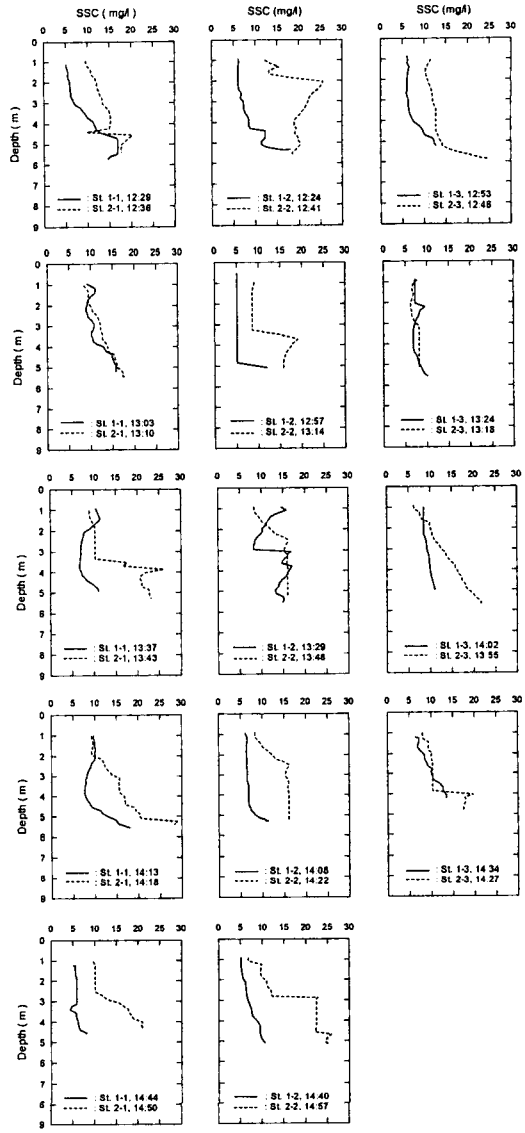

Fig. 6. SSC profiles at the paired front and rear sites of the silt screen on July 10, 2001.

zones than 3 m of the screen depth are markedly distinguished especially at the downstream, which may result from resuspension of bottom sediment near the silt screen. Averages of depth-averaged SSC at the upstream and downstream sites are about 8.9 mg/l and 14.2 mg/l, respectively.

According to the results presented above, it is needed to discuss on the relative magnitudes of current speeds at site A1, A2 and S, generation of SSC peaks, and the possible influence of the screen on the related processes.

4. DISCUSSION

4.1 Influence of the Silt Screen on Current and Suspended Sediment Concentration

Temporal variations of current speeds at sites A1, A2 and S for 24 hours are shown in Fig. 7 with tidal curve at S. The relative magnitudes of current speed of Fig. 7 can be distinguished by tidal phase as shown in Table 3. Current speed at A2 is higher than that at A1 by about 10 cm/s during food period, while vice versa during ebb period. Near-bed speeds at S are comparable to the speed at 3 mab of A1 during flood tides and A2 during ebb period, respectively.

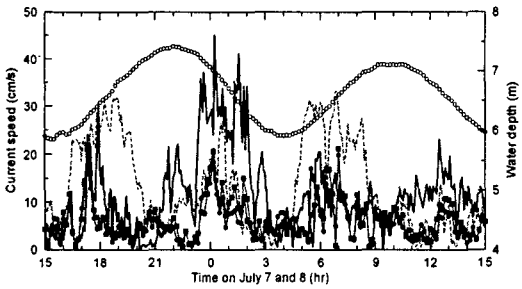

Fig. 7. Temporal variations of current speeds at 3 mab of sites A1 (bold solid line) and A2 (bold dotted), at 25 cmab (line with filled circles) and 50 cmab (with open square) of site S. Open circles mean water depth at S.

Table 3. Tidal phase-averaged current speeds

Tidal Phase	Phase-averaged Current Speed (cm/s)				
	S			A1	A2
	25cmab	35cmab	50cmab	3mab	3mab
Flood I	5.23	5.33	5.74	7.59	16.68
Flood II	6.93	7.02	6.99	9.03	18.32
Flood Averaged	6.08	6.17	6.36	8.31	17.50
Ebb I	6.44	6.76	7.09	19.50	9.85
Ebb II	4.01	4.17	4.89	11.80	5.41
Ebb Averaged	5.23	5.46	5.99	15.65	7.63

Characteristics of these relative magnitudes can be thought to be caused by the silt screen. The conceptual drawing of the related processes is shown in Fig. 8. As seawater passes through the vertical section from the screen bottom to the seabed (hereinafter referred to as *'Venturi section'* following the concept of a Venturi tube with a narrow constriction) it speeds up. Turbulence intensity near the Venturi section (VS) should be

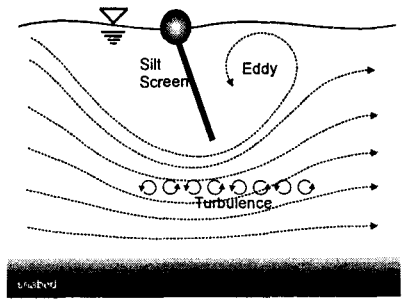

Fig. 8. Conceptual drawing of current fields near a silt screen.

enhanced and eddies of considerable size may be generated in the upper section of the rear. Hence, the current speed and profile at the downstream feeling the VS effect could be largely different from that at the upstream of the same distance.

In this context, the potential that suspended sediments cannot be settled down around the silt screen due to the VS effect should be noted, which means a silt screen may not have any efficiency at all in reducing the spreading of sediment plumes. Furthermore, unless there is a considerable care, the seabed near a silt screen can be eroded, which should be the worst if the bed is highly contaminated.

Stepwise sudden increases of SSC near the screen depth at the downstream sites shown in Fig. 6 presumably result from the VS effect. In fact, the silt curtain in the study area plays adverse effect by 60% if the efficiency is assessed by only the averages of depth-averaged SSCs not SS flux.

However, the higher SSC of the downstream does not mean the higher SS flux that may be a strong evidence of the erosion in the area of the VS. Considering the relative magnitudes of current speeds at A1 and A2, the fluxes may be comparable. The efficiency of the silt screen in terms of SS flux will be discussed.

4.2 SSC near the Silt Screen in a Storm Period

As mentioned above, the SSC peaks in the period from 09:00 on July 6 to 04:00 on July 8 cannot be explained by normal hydrodynamic forcing or dredging especially on July 7 when none of the dredgers worked.

Another important forcing which should be taken into account is wave. Since 1999, the KORDI has been monitoring wave characteristics at site DW in Fig. 1 of

about 4 km southward from the silt screen. The results during early July in 2001 (Fig. 9) indicate that the SSC peaks from July 6 to 7 were generated by wave-induced bed shear stress.

Correlation between significant wave heights measured by a directional wave rider buoy at site DW and those by a pressure gauge at site S is shown in Fig. 10, some deviations in which might be due to locally generated small period waves.

Wave height at A1 can be assumed by the equation in Fig. 10 because site S is just 30 m northward from A1. If the silt screen contributes on wave damping, wave height at A2 may be higher than that at A1. However, according to the experiments of Bruun (1989) shown in Fig. 11, a total of about 90% of incident wave energy is transmitted through the opening of the screen, where the screen depth is half of the water depth. Hence wave height at A2 also can be obtained by the regression formula.

Based on the data, the temporal variation of wave-induced bed shear stress (τ_w) calculated by the equations of Jonsson (1966) and Hunt (1979) at A1 during the storm period is shown in Fig. 12 with current-induced bed shear stresses (τ_c) at A1 and A2 by the equation of van Rijn (1989), water depth at A1, and SSCs at A1 and A2. In the calculation of τ_c, the zero-velocity level is assigned as 0.05 cm which is the average of the values

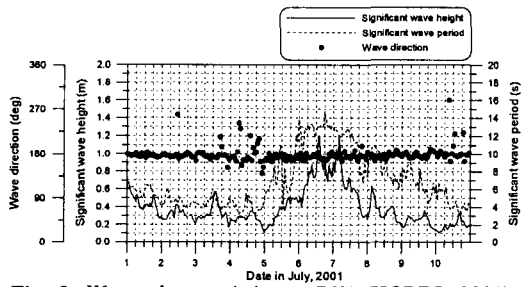

Fig. 9. Wave characteristics at DW (KORDI, 2001).

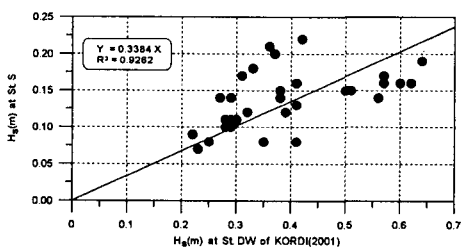

Fig. 10. Correlation between significant wave heights at sites DW and S.

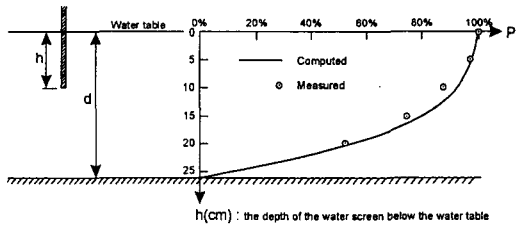

Fig. 11. Transmission ratio of incident wave energy according to the depth of a water screen; total water depth is 26 cm (Bruun, 1989).

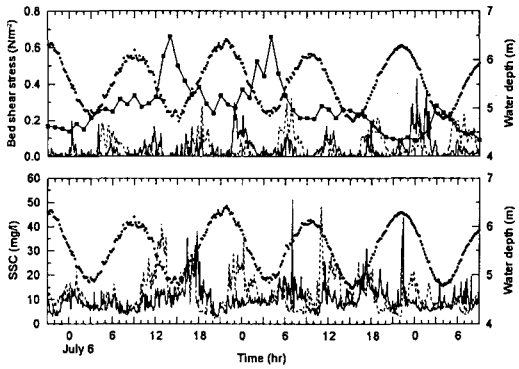

Fig. 12. Temporal variations of wave- and current-induced bed shear stress, water depth and SSC; filled circles and solid line with filled square mean water depth and τ_w at A1, solid lines represent τ_c and SSC at A1 and dotted lines those at A2.

for mud and mud/sand (Soulsby, 1983).

Wave-induced bed shear stress is much higher than τ_c except for the short period including the maximum τ_c of 0.43 N m^{-2} at 00:15 on July 8. The maximum τ_w is 0.66 N m^{-2} occurred at 14:00 on July 6 when significant wave period, water depth and estimated significant wave height were 13 s, 4.92 m and 0.41 m, respectivley.

It can be recognized that SSC peaks are related to the major and minor peaks of τ_w. In connection with the two major peaks of τ_w and associated SSC, however, there are two processes attracting attention. Firstly, due to the fact high concentrated suspension by wave loading is confined in the near bed region (e.g., Bosman, 1982; Mehta, 1988), there is no SSC peak at low water even though the τ_w is considerable. Additionally, the SSC at A2 is much higher than that at A1 in the growing-up periods of the two major peaks of τ_w, while that at A1 is slightly higher in the growing-down periods, although

the time lag between the peak τ_w of the sites must be negligible. It may be explained by the mean diameter of bottom sediments. As shown in Table 2, the mean diameter (62.5 μm) at A1 is much coarser than that (15.6 μm) at A2. Hence it is natural that the SSC at A1 is much lower. Additionally, SSC increases at A1 in growing-down period of flood tide seem to be caused by the advection of the SS entrained in the area of A2.

4.3 Estimation of the Screen Efficiency by Comparison of Suspended Sediment Flux

The behaviors of current speed and SS influenced by the silt screen and waves in the study area are roughly understood as described above. However, the results are not enough to estimate the efficiency of the screen in reducing the spreading of dredging-induced SS plume because the second half period of the AURY monitoring has no data of A1, and current measurements were not concurrently associated with the cruise profiling of the SSC at 6 sites near the screen.

Temporal variations of calculated SS fluxes at 3 mab at A1 and A2 are shown in Fig. 13. Due to no dredging in the storm period and no data at A1 in the latter half period, the only possible period for comparing the fluxes of the plume SSC generated by dredging is the second ebb on July 6 when all the 3 dredgers were working. It may be useful to compare them with the fluxes during the ebb period of mild sea state without dredging.

From Table 4 showing calculated SS fluxes at 3 mab of the two sites during the mentioned two periods, it is recognized that the southward net fluxes during the normal ebb period are comparable, while the flux of A2 is lower than that of A1 by 55.5% in the dredging period.

It should be more valuable to roughly estimate the screen efficiency by vertical integration of SS fluxes with some proper assumptions, although profiling of current speed was not associated with SSC profiling on July 10.

Vertical integrations of the SS fluxes of sites 1-2 and 2-2 can be roughly estimated with measured SSC profiles, current speed at A2 and following assumptions based on the current patterns shown in Fig. 7:

1) Velocity profile at A1 can be roughly fitted by applying the near-bed currents at S concurrently measured.

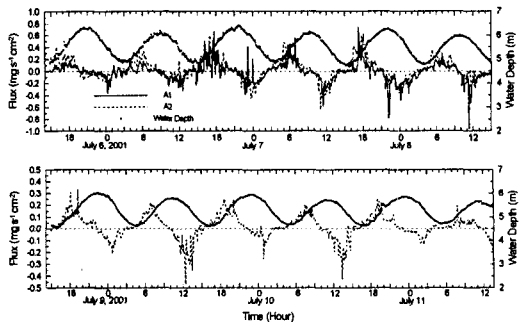

Fig. 13. Temporal variations of SS fluxes at 3 mab of sites A1 and A2 (dotted line).

Table 4. Comparison of SS fluxes per unit area (g s^{-1} cm^{-2}) at 3 mab of sites A1 and A2 according to dredging condition (sign means flux direction)

Period& Site / Flux dir.	w/o Dredging 20:30 07/05-03:30 07/06		Dredging 09:30 - 15:00 07/08	
	A1	A2	A1	A2
Northward	0.145	0.204	0.000	0.013
Southward	-1.342	-1.276	-2.885	-1.297
Net	-1.197	-1.072	-2.885	-1.284

2) Ebb current profile at A2 are similar to flood profile at A1.
3) Velocity profiles at sites 1-2 and 2-2 are assumed to be the same as the approximated profiles at A1 and A2, respectively.
4) The ratio of the current speed at 3 mab of A1 to that of A2 in the ebb period of the cruise profiling of SSC can be approximated by the ratio in the averaged ebb period in Fig. 7.
5) The ratio of current speed at a certain height above the bed to that at 3 mab of A1 or A2 in the cruise profiling period is assumed to be the same as the ratio in the approximated current profiles based on Fig. 7.

In order to approximate the averaged current profiles of A1 and A2 during 2.67-hour SS profiling of the second mid-ebb period on July 10, current velocities at A1, A2 and S for the corresponding periods of Fig. 7 are calculated as shown in Table 5.

Based on the first assumption and the averages at S and A1 in Table 5, the velocity profiles of mid-flood and -ebb periods at A1 are fitted as shown in Fig. 14. However, it should be noticed that the fitted formulae are

Table 5. Averaged current speeds for 2.67 hours of mid-flood and mid-ebb tides of Fig. 7

Tidal Phase	Averaged Speed for 2.67-hour (cm/s)					A1/ A2
	S			A1	A2	
	25cmab	35cmab	50cmab	3mab	3mab	
MF* I	6.46	6.50	6.56	10.53	25.44	0.41
MF II	9.33	9.51	9.53	11.04	25.81	0.43
MF Averaged	7.89	8.00	8.03	10.78	25.62	0.42
ME# I	9.54	10.22	11.31	27.96	14.48	1.93
ME II	4.13	4.28	5.74	12.97	4.42	2.93
ME Averaged	6.84	7.25	8.53	20.47	9.45	2.17

* MF: Mid-flood, # ME: Mid-ebb

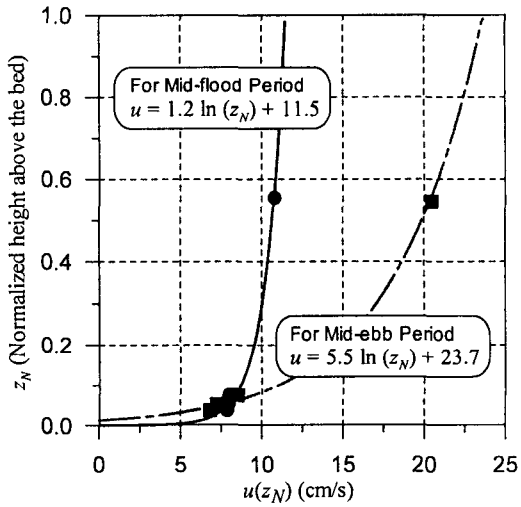

Fig. 14. Velocity profiles fitted to averaged current speeds at A1 for mid-flood and -ebb periods of 2.67 hours of Fig. 7.

not directly applied in integrating SS fluxes at sites 1-2 and 2-2 but just references. The mid-flood profile of A1 in Fig. 14 is referred to the mid-ebb profile of A2 according to the second assumption.

Verical integrations of SS fluxes per unit width at sites 1-2 and 2-2 are summarized in Table 6. The maximum

Table 6. Approximated SS fluxes at sites 1-2 and 2-2 for the dredging period on July 10

Time	SS flux (mg cm^{-1} s^{-1})		Flux Ratio
	Site 1-2	Site 2-2	
12:32	43.99	36.62	0.83
13:06	37.54	38.37	1.02
13:59	56.37	39.04	0.69
14:15	74.11	66.28	0.89
14:48	43.77	63.11	1.44

efficiency of the silt screen is approximated as 30% at about 14:00. However, it should be noticed that the adverse effect still occurs. According to the calculation based on the above assumptions, the averaged efficiency is only 5 %.

5. CONCLUSIONS

By field measurements in a microtidal coastal area where silt screens had been installed and 3 mechanical dredgers were working, and introduction of some approximations based on the results, a few phenomena have been understood:

1) Current speed at about 30 m downstream of the silt screen is about the half of that at same distance of the upstream.
2) Vertical gradient of the current velocity of the upstream is steeper than that of the downstream.
3) Even for a relatively weak storm period, SSC increases up to the value caused by dredging. Thus, preliminary study on the efficiency and necessity of a silt screen should be carried out with consideration of wave climate in a planned dredging term.
4) Section-averaged SSC of the downstream is higher by 60% than that of the upstream, which means the silt screen in the study area plays adverse effect in the aspect of reducing SSC generated by dredging.
5) Maximum efficiency of the silt screen in terms of the integration of SS flux is about 30%, while the average is only 5%.

For deep understanding of the influence of a silt screen on the current structure and associated behavior of suspended sediment and bed property as well as the movement of the silt screens, more detailed field measurements are required.

Considering the above results, the silt screen of fixed hanging type of which screen depth is about the half of water depth does not play a mitigation measure against reducing the spreading of the SS plumes generated by dredging in the study area where the mean current velocity ranges about 20 to 30 cm/s.

In order to establish a more general guidance on the efficiency of silt screens, however, further studies should be carried out.

ACKNOWLEDGEMENTS

This study was supported by the Ministry of Maritime Affaires and Fisheries. The authors are grateful to Mr. W. D. Baek and Mr. Y.C. Kim of KORDI for their devotional contribution to the field measurements.

REFERENCES

Bosman, J., 1982. Concentration measurements under oscillatory motion, *Report M1695-II*, Delft Hydraulics, The Netherlands.

D&A Instrument Company, 1991. Instruction manual OBS-1 & 3.

Hunt, J.N., 1979. Direct solution of wave dispersion equation, *J. Waterways, Port, Coastal Ocean Div.*, ASCE, 105(WW4), pp. 457-459.

Jensen, A., 2001. Environmental investigation, *Dredging and reclamation*, N.J. Gimsing and C. Iversen eds., The Øresund Technical Publications.

Jin, J.-Y., Hwang, K.C., Park, J.S., Lee, K.S., Yum, K.D. and Oh, J.K., 2003a. Development of a programmable suspension sampler to improve the monitoring of sediment-transport processes, *Proc. Coastal Sediment '03*.

Jin, J.-Y., Song, W.O., Maeng, J.H., Ahn, H.D., Chae, J.W., Park, J.S., Oh, Y.M. and Oh, J.K., 2003b. A draft guidance on the installation and maintenance of silt screens, *Proc. Conf. Korean Soc. Coastal and Ocean Engrs.*, this volume. (in Korean)

John, S.A., Challinor, S.L., Simpson, M., Burt, T.N. and Spearman, J., 2000. Scoping the assessment of sediment plumes from dredging. *Pub. No. CIRIA C547*, Construction and Industry Research and Information Association of the UK.

KORDI, 2000. Restoration of the eastern marginal environment of the Yellow Sea (REYES) : Creation and restoration of environmentally sustainable tidalflat (CREST), *BSPE 00785-00-112-2*. (in Korean with English summary)

KORDI, 2001. Maintenance of a directional wave rider for breakwater construction of Busan New Port, *BSPI 329-00-1362-2*. (in Korean)

Mehta, A.J., 1988. Laboratory studies on cohesive sediment deposition and erosion, *Physical Processes in Estuaries*, J. Dronkers and W. van Leussen eds., Springer-Verlag, Berlin, Germany.

Ministry of Maritime Affairs and Fisheries, 2001. Studies on the estimation of turbidity generated by dredging and performance of silt screens (I). (in Korean with English summary).

Mouchel Asia Ltd., 2002. Infrastructure for Penny's Bay Development-Contract 1 / Quarterly environmental monitoring and Audit (EM&A) *Report (No.2) March 2002-May 2002-Rivision A*.

Ooms, K., 1997. Disposal and capping of contaminated sediments-the Hong Kong solution, *Proc. the CEDA Dredging Days*, Amsterdam, The Netherlands.

Reine, K.J., Dickerson, D.D. and Clarke D.G., 1998. Environmental windows associated with dredging operation, *Technical Note, DOER-E2*, U.S. Army Engineer Research and Development Center, Vicksburg, MS.

Shaw, J. K., Whiteside, P.G.D. and Ng., K.C., 1998. Contaminated mud in Hong Kong: A case study of contained seabed disposal, *Proc. 15th World Dredging Congress*, World Dredging Association, Las Vegas.

Soulsby, R.L., 1983. The bottom boundary layer of shelf seas, *Physical Oceanography of Coastal and Shelf Sea*, B. Johns ed., Elsevier Science Pub., Amsterdam, The Netherlands.

van Rijn, L.C., 1989. Handbook of sediment transport by currents and waves, *Report H461*, Delft Hydraulics, Delft, The Netherlands.